Sains Malaysiana 52(4)(2023): 1231-1242
http://doi.org/10.17576/jsm-2023-5204-15

Synthesis, Characterisation and Binding Evaluation of New 6-Amidinoindole Compound as the Potential Heme Binder

(Sintesis, Pencirian dan Penilaian Pengikatan Sebatian 6-Amidinoindol Baharu sebagai Pengikat Heme Berpotensi)

NORAISYAH ABDUL KADIR JILANI[1], NATSUHISA OKA[2,3], KAORI ANDO[2] & SITI AISHAH HASBULLAH[1,*]

[1]*Department of Chemical Sciences, Faculty of Science and Technology, Universiti Kebangsaan Malaysia, 43600 UKM Bangi, Selangor Darul Ehsan, Malaysia*
[2]*Department of Chemistry and Biomolecular Science, Faculty of Engineering, Gifu University, Gifu 501-1193, Japan*
[3]*Institute for Glyco-core Research (iGCORE), Gifu University, Gifu 501-1193, Japan*

Received: 11 March 2022/Accepted: 6 March 2023

ABSTRACT

In this study, the new compound 6-amidinoindole **3** were synthesized by hydrogenating the amidoxime unit in a high yield. The compound was characterized by FTIR, ^{1}H NMR, ^{13}C NMR and ESI-MS. The binding of the compound towards heme was evaluated using absorption spectroscopy. The studies found that the association constant (log K) is 3.90. The binding strength indicated the ligand's possibility to interact significantly with heme and acted as a binder to the malaria parasite. *In silico* hemozoin docking was performed to gain insight into the mode of action. The docked score is -8.3 kcal/mol, indicated the possible inhibition of hemozoin. This study could serve as the basis for the future development of malaria sensors and antiplasmodial activity.

Keywords: Amidino; heme binding; indole; malarial molecular target; synthesis

ABSTRAK

Dalam kajian ini, sebatian 6-amidinoindol **3** baharu telah disintesis melalui penghidrogenan unit amidoksim dan hasil yang tinggi telah diperoleh. Sebatian ini telah dicirikan oleh FTIR, ^{1}H NMR, ^{13}C NMR dan ESI-MS. Pengikatan sebatian terhadap heme telah dinilai menggunakan spektroskopi serapan. Kajian mendapati bahawa pemalar pengikatan (log K) ialah 3.90. Kekuatan pengikatan menunjukkan kebolehan ligan berinteraksi dengan heme secara signifikan dan juga bertindak sebagai pengikat kepada parasit malaria. Mengedok hemozoin secara *in silico* dilakukan untuk mendapatkan gambaran lebih dalam tentang cara kerja. Dok skor ialah -8.3 kcal/mol yang menunjukkan kemungkinan berlakunya perencatan hemozoin. Kajian ini boleh menjadi asas untuk pembangunan sensor malaria dan aktiviti antiplasmodial pada masa hadapan.

Kata kunci: Amidino; indol; pengikatan heme; sasaran molekul malaria; sintesis

INTRODUCTION

Malaria is a major health disease caused by parasites transmitted through the Anopheles mosquito bite (Kumar et al. 2012). Worldwide, malaria cases count to 241 million in 2020, while the death number is 627000 (WHO 2021). Malaysia is not yet certified to be malaria-free (Sam et al. 2022). The concern nowadays is that the currently available drugs have developed resistance to the parasites (Ashley et al. 2014; Paloque et al. 2016). New and efficient drugs are needed to overcome this global issue (Radzuan et al. 2021). Natural organic compounds such as artemisinin and quinine derived from plants have been explored to give good antimalarial activity (Newman & Cragg 2007).

The malaria parasite destroys human red blood cells and releases hemozoin (malaria pigment) into the

bloodstream for detoxification (De Villiers & Egan 2021; Kapishnikov et al. 2021). The blockage of this process is essential to stop the parasite's survival. The mechanism targets the heme and forms heme-drug adducts, which can cause a cytotoxic environment for the parasite (Openshaw et al. 2021). Subsequently, this leads to the blocking of parasite growth (Olafson et al. 2017). Therefore, heme binding with drugs is ultimately crucial in developing antimalarial drugs.

Thus, heme binding studies have been explored extensively. The interactions are mainly non-covalent bonding such as π-π stacking, hydrogen binding, hydrophobic, and hydrophilic interaction. Interestingly, a known hemozoin inhibitor chloroquine also possesses π-π stacking interactions with the hemozoin (Bailly 2021). Another study by Roman et al. (2010) demonstrated the potential of the triazole derivative to interact with heme strongly via hydrophobic binding. Therefore, the binding studies are necessary to understand the mode of action between heme and ligand.

Indole alkaloids are isolated from plant and marine sources and have massive impacts on the medical field (Pindur et al. 2001; Taher et al. 2022). Currently, indole compounds, namely vincristine, reserpine, physostigmine and ajlamine, are used in the remedial treatments of anticancer, antihypertensive, cholinesterase inhibitor and antiarrhythmic agents correspondingly (Omar et al. 2021). Indole scaffolds are usually associated with potent biological activities, including anticancer, antiviral, antimalarial, antidepressant, and antileishmanial (Kaushik et al. 2013). In addition, the preclinical trials of cipargamin III (NITD609, KAE609), a new class of antimalarials based on oxindole derivative, have been recently discovered (Turner 2016).

Therefore, in this study, we synthesized a new 6-amidinoindole compound and elucidated the product by FTIR, NMR, and mass spectroscopy. Heme binding interaction of the compound was performed by UV-vis spectroscopy to gain deep knowledge of the mechanism of action and the binding association constant (log K). The study indicated the potential of the compound to target the malaria parasite.

Materials and Methods

Chemicals and Instrumentation

Reagents are commercially available and used without purification. Dry organic solvents were readied accordingly before use. The thin layer chromatography (TLC) and column chromatography were carried out using Merck precoated silica gel 60 (No. 5715) and Kanto silica gel 60N (spherical, neutral, 40-50 or 63-210 μm), respectively. NMR spectra (^{1}H, ^{13}C) were performed in DMSO-d_6 using the JEOL JNM-ECS-400 spectrometer. FTIR spectrum of the compound was recorded between 4000-400 cm^{-1} using PerkinElmer 400 FT-IR spectrometer in attenuated total reflectance (ATR) mode. The mass spectrum was collected on Waters Xevo Q-Tof mass spectrometer (ESI-TOF). The absorption spectra were measured using Shimadzu UV 1800 spectrophotometer.

Synthesis of 6-amidoximeindole **(2)**

6-cyanoindole **1** (0.43 g, 3.0 mmol) was dissolved in a cryotube containing dry dioxane (3 mL). Hydroxyl amine aqueous 50% (1.10 mL, 18.0 mmol) was added to the solution and heated at 80 °C for 5 h (Scheme 1). The solution was cooled to room temperature, and the solvent was evaporated under reduced pressure. Purification was performed using silica column chromatography with 0-5% methanol in dichloromethane to afford amidoxime **2** (tan solid, 68%), and amide **2a** (tan solid, 16%). The method was modified from the literature that used hydroxylamine hydrochloride salt and triethylamine base. The NMR spectrum was in accordance with those reported (Congdon et al. 2021). **2** (tan solid, 68%): ^{1}H NMR (400 MHz, $(CD_3)_2SO$) δ_H 11.20 (br, s, 1H), 9.44 (s, 1H), 7.70 (s, 1H), 7.49 (d, J = 8.4 Hz, 1H), 7.38 (t, J = 2.8 Hz, 1H), 7.34 (dd, J = 8.4, 1.6 Hz, 1H), 6.43-6.42 (m, 1H), 5.73 (s, 2H).

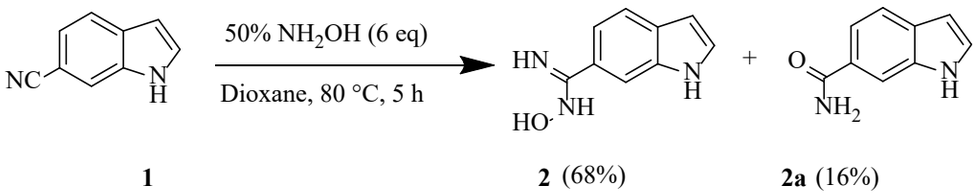

1 **2** (68%) **2a** (16%)

SCHEME 1. Synthesis of 6-amidoximeindole **2** and 6-indolylamide side product **2a**

SYNTHESIS OF 6-AMIDINOINDOLE **(3)**

Amidoxime **2** (0.18 g, 1.0 mmol), Pd/C (0.11 g, 0.1 mmol/10 mol%) and dry ethanol (10 mL) were added to the autoclave reactor (Scheme 2). The reactor was closed securely, exposed with hydrogen and charged with 3 atm pressure. The reaction proceeded at room temperature and took 4 days to achieve completion. The mixture was filtered through celite and washed efficiently with ethanol to remove the catalyst. The filtrate was evaporated under vacuum to obtain amidino **3** (tan solid, 87%). IR (ATR, υ_{max}/cm^{-1}): 3428 (N-H), 3060 (C-H), 1646 (C=N), 1545 (C=C), 1350 (C-N); ^{1}H NMR (400 MHz, $(CD_3)_2SO$) δ_H 7.84 (s, 1H), 7.54 (d, J = 8 Hz, 1H), 7.44-742 (m, 2H), 6.46 (s, 1H); ^{13}C NMR (400 MHz, $(CD_3)_2SO$) δ_C 164.4, 135.3, 129.1, 128.6, 127.4, 119.1, 117.8, 110.2, 101.1; HRMS (ESI-TOF) m/z: $[M + H]^+$ calcd for $C_9H_{10}N_3^+$ 160.0869; found 160.0865.

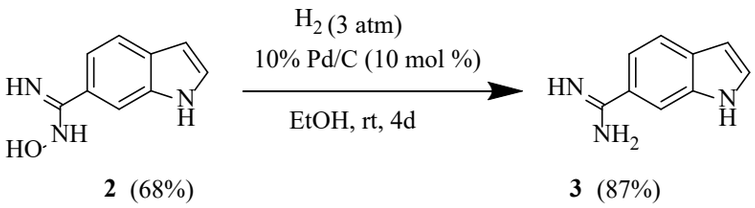

2 (68%) **3** (87%)

SCHEME 2. Synthesis of final product 6-amidinoindole **3**

BINDING EXPERIMENT WITH HEMIN

The hemin binding studies were performed according to the literature (Egan et al. 1997). A 0.5 mM (pH 7.5) hemin stock solution was prepared by dissolving 3.26 mg hemin chloride in 10 mL DMSO. The 8 µM hemin working solution was prepared from a mixture of 160 µL of hemin stock solution, 5 mL of deionized water, 3.84 mL of DMSO and 1 mL of 0.2 M tris buffer (tris(hydroxymethyl)aminomethane). The reference cell contained DMSO-aqueous (40% v/v) solutions of 5 mL of deionized water, 4 mL of DMSO and 1 mL of 0.2 M tris buffer. The ligand aliquots of 5-25 µL were added to the working and reference solutions to remove the absorbance of the compound. The addition of ligand was up to 160 µM. The absorption spectra were recorded after 1 min to allow the hemin-ligand solutions to stabilize. The association binding constant was established using the equation $A = (A_0 + A_\infty K[C])/(1 + K[C])$ and fitted the 1:1 complexation model using the nonlinear least square fitting. A_0 is the absorbance of hemin; A_∞ is the absorbance of hemin-ligand adduct at the saturation; A is the absorbance of hemin-ligand at each titration point; and K is the association constant. GraphPad Prism 9.4.1 software was used to calculate the binding constant of the titration curve using the nonlinear regression curve analysis.

MOLECULAR DOCKING

The geometry of the 6-amidinoindole **3** has been optimized on Gaussian 09 program using Beck's three-parameter Lee Yang Parr density functional theory model (B3LYP) basis set 6-311G+ (d,p). AutoDock Vina was used to dock the ligand with hemozoin. The hemozoin crystal was obtained from Cambridge Crystallographic Data Centre (CCDC) (XETXUP01) and employed as a biomolecular receptor. The hemozoin crystal supercell 2 × 2 × 2 cell lattice was formed using Vesta software (Momma & Izumi 2008). Supercell is the extension of the single unit cell. The grid box of size 80 × 126 × 112 and coordinates of x=10.221, y=14.365 and z=9.067 were used for the molecular docking. The Auto Dock result was visualized using BIOVIA Discovery Studio.

RESULTS AND DISCUSSION

SYNTHESIS OF INDOLYLAMIDOXIME, INDOLYLAMIDE AND INDOLYLAMIDINO

Owing to the outstanding properties of the indole and amidine scaffold, we are interested to synthesised new amidine based indole compound through the nitrile functional group modifications. The synthetic modification was possible due to the electrophilic character of the nitrile carbon. Firstly, the nitrile group was converted to amidoxime unit via hydroxyl amine

addition reaction followed by the hydrogenation to amidine unit.

The formation of intermediate 6-amidoximeindole has previously been reported by Congdon et al. (2021) utilising hydroxylamine hydrochloride in the presence of triethylamine base in ethanol at 80 °C for 12 h. The yield obtained was high, 91% according to the reported procedure. However, in this study, we synthesised intermediate 6-amidoximeindole by reacting the 6-cyanoindole with 50% aqueous solution of hydroxylamine in dry dioxane at 80 °C for 5 h to afford moderate yield of intermediate indolylamidoxime **2** 68% and small undesired indolylamide **2a** 16%. Although the yield was moderate, the time taken for completion was shorter only 5 h without the use of base compared to previous procedure. Therefore, the method was recommendable to be explored in the future.

Fundamentally, the reaction of arylnitrile to arylamidoxime always produced arylamide (side product) (Srivastava et al. 2009). Thus, it has taken interest of the researchers to minimize the production of side product using different techniques. Additionally, the mechanism of formation of amidoxime and amide side product was studied extensively by Vörös et al. (2014) using kinetic and thermodynamic analysis in order to properly addressed the mechanism involved. The plausible mechanism was explained in detailed the next subtopic.

For the formation of new 6-amidinoindole **3**, it involved the conversion of amidoxime to amidine unit. The method employed hydrogen gas at 3 atm over palladium on carbon in ethanol and yielded 87% product. This attractive method was widely used due to mild conditions such as low pressure and at room temperature. All the products formation was confirmed using spectroscopy and analytical methods.

The ^{1}H NMR spectrum of amidoxime intermediate **2** was in line with the literature but with a slight difference in the chemical shift (Congdon et al. 2021). The spectrum in this study was more detailed as the appearance of proton labile can be observed (Figure 1). The amine proton -NH of the indole ring was demonstrated at 11.20 ppm as a singlet peak. The signal is the most downfield due to the acidic proton nature. The hydroxyl proton -OH and primary amine proton -NH_2 of the amidoxime group resonated at 9.44 and 5.73 ppm, respectively.

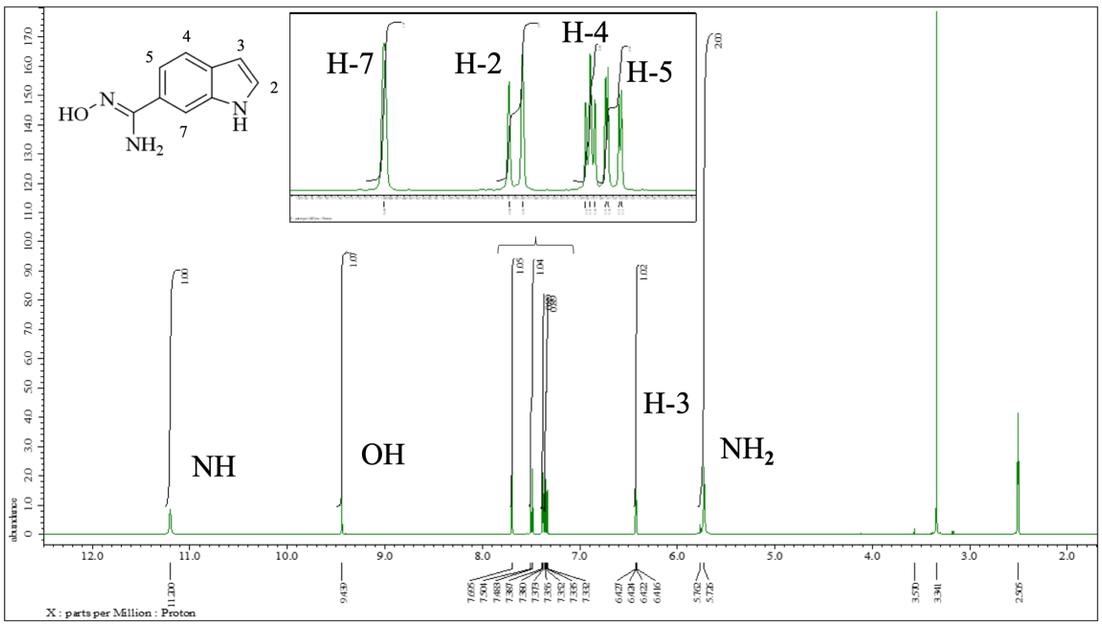

FIGURE 1. ^{1}H NMR spectrum of 6-amidoximeindole **2**

Compound **3** was characterized by infrared spectroscopy to confirm the formation of the product. The spectrum exhibited the functional groups of N-H at 3428 cm^{-1} corresponds to the NH of indole and amidino groups (Figure 2). The C=N stretching also confirmed the amidino group's existence at 1646 cm^{-1} (Kollipara et al. 2003). The frequencies of C-H, C=C and C-N, were observed at 3060, 1545, and 1350 cm^{-1}. These vibrational peaks were in accordance with the literature on indole derivatives (Melo et al. 2021).

Further elucidation of the compound was conducted using NMR spectroscopy. The ^{1}H NMR spectrum of the 6-amidinoindole **3** illustrated the appearance of all the aromatic protons of the indole scaffold (Figure 3(a)). Meanwhile, the proton of NH indole, NH amidino and NH_2 amidino were not presented in the spectrum due to the labile characteristic of the proton. Labile proton causes peak broadening and peak disappearance because of the fast exchange between compound protons and water protons (Gil et al. 2013). The aromatic proton H-3 was the most shielded with regard to the NH group of indole that distributed fewer electrons at position 3. However, the signal was observed as singlet due to the fast exchange of the protons; supposedly, the peak signal doublet of doublet was expected. The aromatic proton H-7 demonstrated a singlet peak at 7.84 ppm as no neighbouring proton exists. Duplet peak at 7.54 ppm corresponds to the H-2 proton that coupling to one proton, H-3. While the protons H-4 and H-5 resonated between 7.44-7.42 ppm as an overlapping multiplet.

The ^{13}C NMR spectrum of the final product showed the presence of resonance carbon at 164.4 ppm, the furthest downfield region referred to as the carbon of amidino (Figure 3(b)). This confirms the success of the reduction reaction (hydrogenation) from amidoxime group $C(NH_2)$(N-OH) to amidino group $C(NH_2)$(NH). The quaternary aromatic carbons, C7a, C3a and C6, were observed as a less intense signal because of the weaker Nuclear Overhauser Effect (NOE) (Furrer 2021). Quaternary carbon C7a was located in the most deshielded area because the nuclei were attached to the electronegative group NH. This was followed by quaternary carbon C3a and C6, two and three bonds to the NH group. The aromatic carbons were demonstrated in the range of 101.1 to 127.2 ppm. The most deshielded aromatic carbon was possessed by C2 at 127.2 ppm that attached to the electronegative NH group indole, and has amidine group at position 6 (Alagona, Ghio & Monti 1998). Chemical shift at 119.4 ppm was referred to the carbon C4 due to the resonance of electron by amidino deactivating group that facilitates the electron donation at meta position C4. In addition, carbon C5 and C7 were ortho to the amidino group but differed in position from the NH indole. In which carbon C5 is at the para position and carbon C7 is at the ortho position. Thus, carbon C5 was more deshielded than carbon C7 as the electron donation was the greatest at the para site. Carbon C3 resonated at 101.1 ppm due to the resonance stabilization of the pyrrole ring.

The MS analysis supported the formation of 6-amidinoindole, $C_9H_{10}N_3^+$. From the spectrum, the molecular ion peak $[M + H]^+$ calculated and observed was in good agreement, at 160.0869 and 160.0865, respectively (Figure 4).

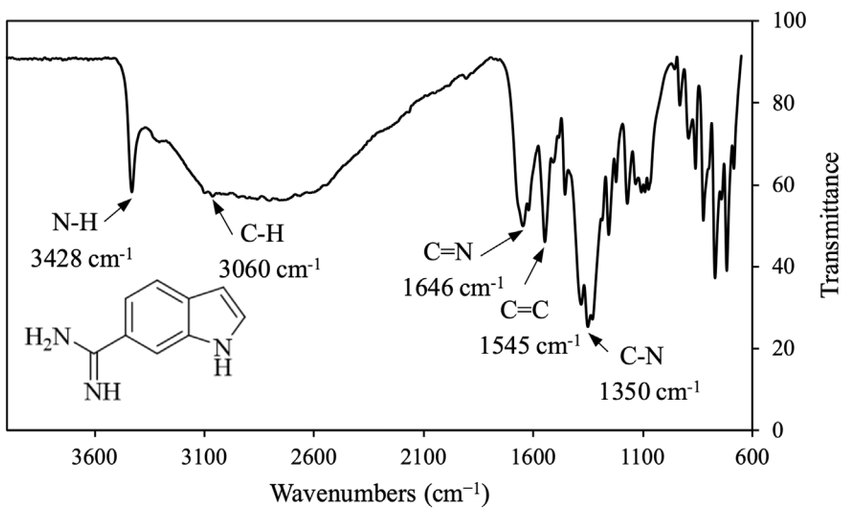

FIGURE 2. FTIR spectrum of 6-amidinoindole (**3**)

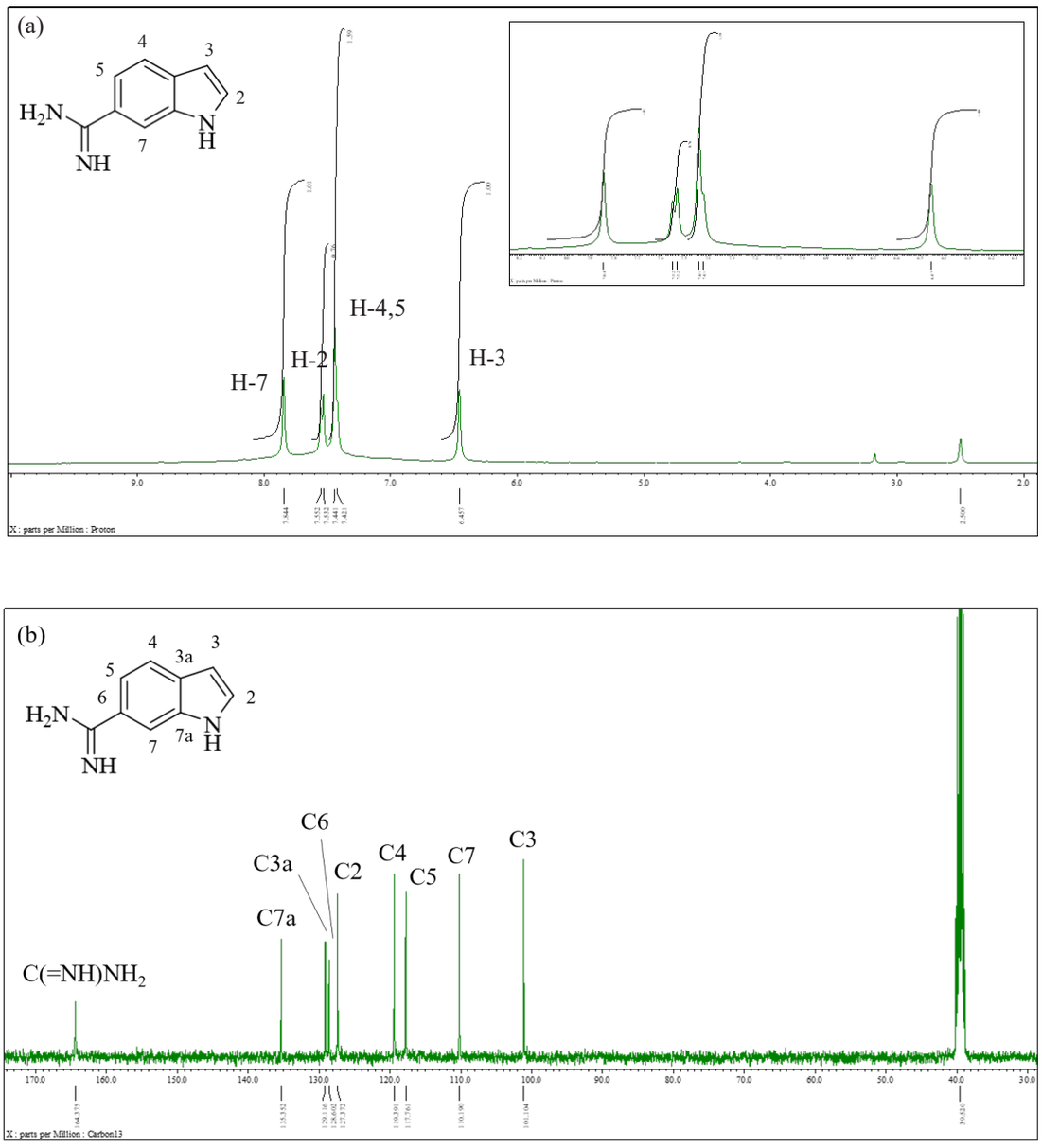

FIGURE 3. (a)^{1}H NMR and (b) ^{13}C NMR spectrum of 6-amidinoindole (**3**)

A PLAUSIBLE MECHANISM FOR THE SYNTHESIS OF 6-AMIDINOINDOLE

The formation of the 6-amidoximeindole **2**, 6-indolylamide **2a** and 6-amidinoindole **3** was described in the present work. The synthesis of 6-amidoximeindole produced a small undesired side product of 6-indolylamide. There is also a study on reducing the undesired amide product (Stephenson, Warburton & Wilson 1969). Hydroxylamine is an ambident nucleophile, which can perform nucleophilic attacks from two sites, nitrogen or oxygen atom. This result in the formation of more than one product.

Firstly, the nucleophilic character of the nitrogen atom of hydroxylamine attacked the nitrile's carbon atom, followed by the intramolecular proton transfer to provide amidoxime isomer of iminohydroxylamine

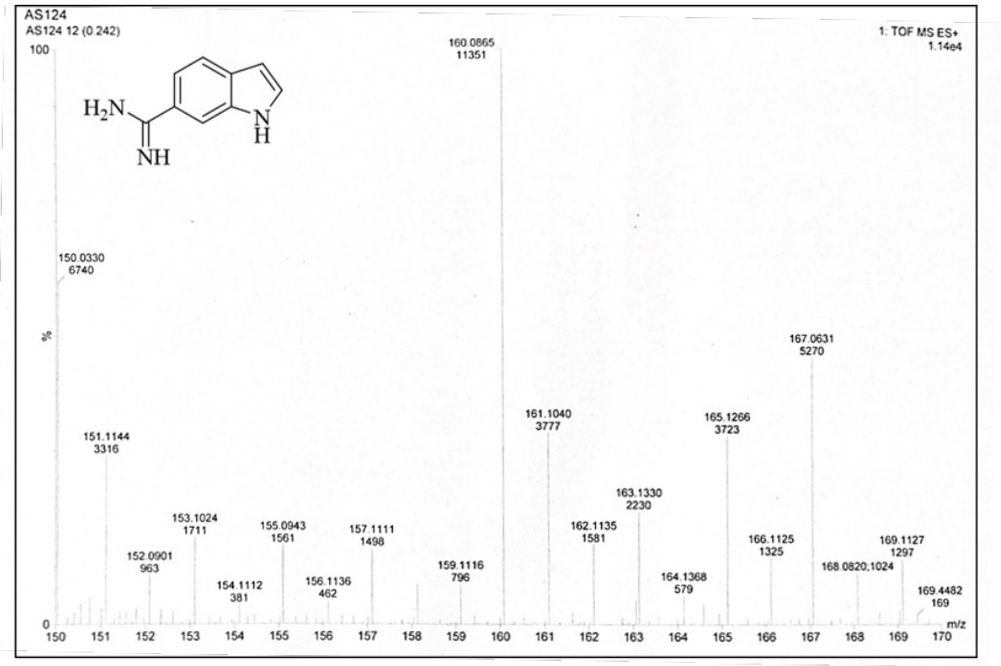

FIGURE 4. Mass spectrum of 6-amidinoindole (**3**)

-C(=NH)(NH-OH). This isomer then undergoes tautomerisation to form the most stable and dominant (Z)-amidoxime **2** product (Scheme 3(a)) (Sahyoun et al. 2019).

The mechanism for the formation of undesired amide **2a** is illustrated in Scheme 3(b). Primarily, the nucleophilic character of the oxygen atom of hydroxylamine attacks the carbon atom of the nitrile and undergoes protonation to afford carboximidate intermediate -C(=NH)(O-NH_2). Subsequently, an additional hydroxylamine nitrogen atom attacked the NH_2 group and yielded side product amide **2a** and unstable NH_2NHOH (**NNO**). The previously reported additional reaction with hydroxylamine affords amide **2a** and unstable NH_2NHOH (**NNO**) or NH_2ONH_2 (**NON**) (Stephenson, Warburton & Wilson 1969). However, a study by Vörös et al. (2014) proved that the more stable side product of the reaction was amide and NH_2NHOH (**NNO**) with regards to the kinetic and thermodynamic studies performed.

The plausible proposed mechanism of catalytic reduction of (Z)-amidoxime unit to amidino unit in the presence of Pd/C is shown in Scheme 3(c). The H_2 bond cleaved in the presence of Pd catalyst and formed bonds each to the metal surface Pd. The hydroxyl group undergo protonation with the positively charged hydrogen forming OH_2^+ group. And then, hydride attacked the nitrogen atom NH followed by the leaving of water molecule afforded the amidino group **3**.

HEME UV BINDING

In order to study the possible mode of interaction between ferriprotoporphyrin IX (Fe^{III}PPIX) or hemin, a commercial heme, and ligand, titration studies using absorption spectroscopy were performed. Hemin has an intense Soret band at 399 nm, corresponding to the π-π^* transition of the porphyrin group (Brunet et al. 2012). Upon titration of the ligand, the absorbance gradually decreases by 10% hypochromic at a 20:1 ratio (ligand: hemin). The association constant, log K calculated was 3.90 based on the 1:1 model of hemin-ligand fitted the nonlinear regression curve (Figure 5). The value of the log K is smaller than known heme inhibitors, chloroquine which possesses 5.52 strength (Egan et al. 1997). Meanwhile, the association constant is comparable to and equal to the quinine and mefloquine heme inhibitor, which are 4.10 and 3.90, accordingly (Egan et al. 1997). The association constant is more significant than the copper(I)-chloroquine complex, which is only 3.55 in strength (Villarreal et al. 2022). In summary, the ligand has the potential to target the malaria parasite.

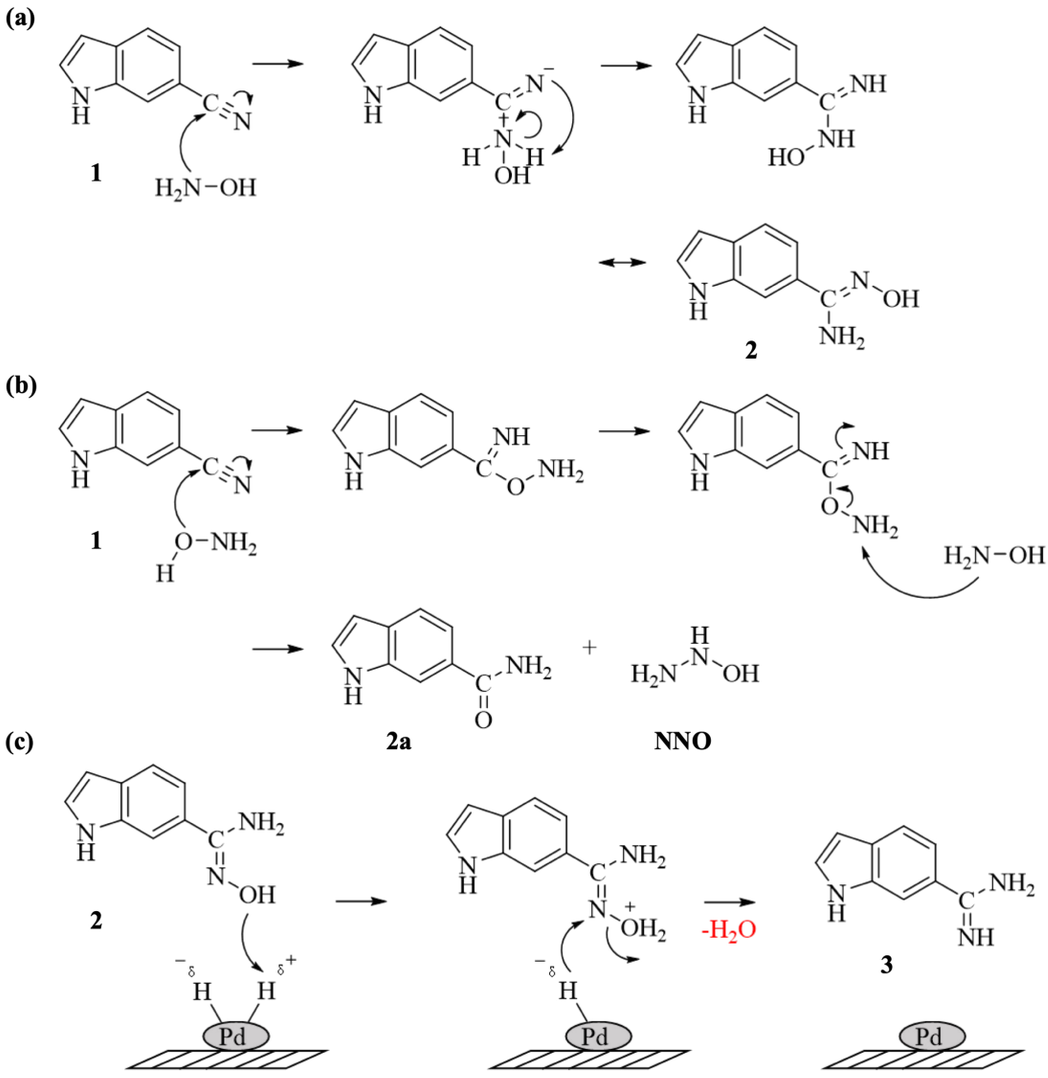

SCHEME 3. (a) Proposed mechanism of the main product, 6-amidoximeindole (b) Proposed mechanism of a side product, 6-indolylamide (c) Proposed mechanism of the final product, 6-amidinoindole in the presence of Pd/C catalyst

IN SILICO STUDIES AGAINST HEMOZOIN

The mechanism of antimalarial activity involves the inhibition of the hemozoin crystallization inside the vacuole of the *Plasmodium* by releasing the toxic heme-drugs adduct, which inevitably leads to parasite death (Buller et al. 2002; Fong & Wright 2013). Hemozoin inhibition is the core target for most antimalarial drugs (Coronado, Nadovich & Spadafora 2014). Therefore, the molecular docking simulation was conducted to gain insight into the possible mechanism of action between 6-amidinoindole **3** and malaria parasites. The molecule was docked against all the surfaces of the crystal lattice of the hemozoin. The 6-amidinoindole **3** docked score was -8.3 kcal/mol (Figure 6). The binding affinity of the simulated ligand was lower than -5 kcal/mol, indicating the favourable interactions of ligand and hemozoin

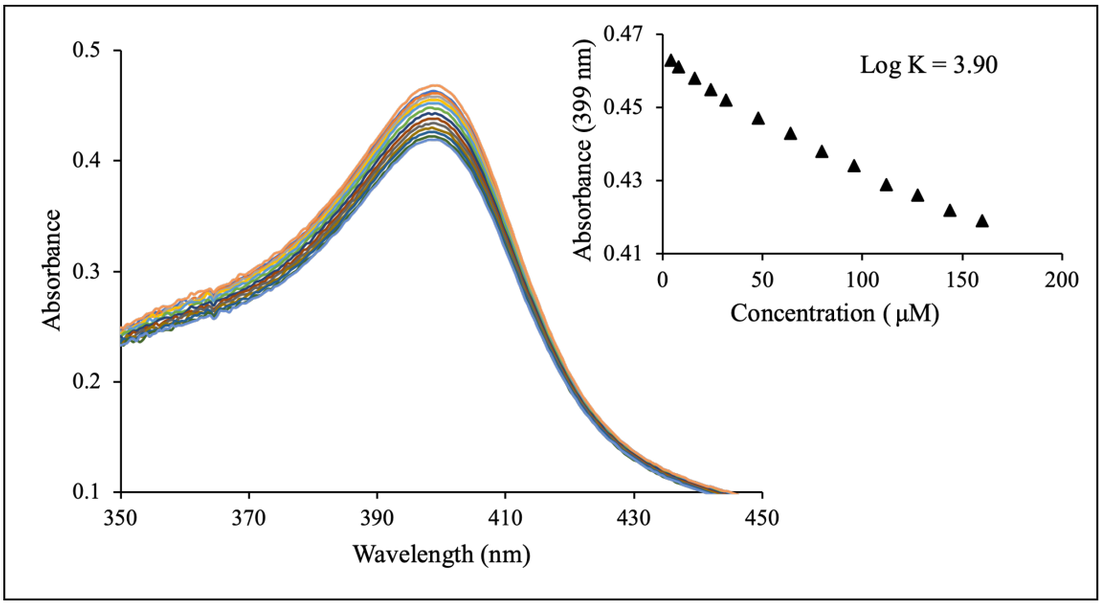

FIGURE 5. Absorption spectra of hemin chloride 8 μM at pH 7.5 upon addition of 6-amidinoindole (up to 160 μM). Inset is the plot of A_{399nm} vs concentration

(Takahashi et al. 2010). Although the docking binding sites involved all of the surfaces of the hemozoin crystal, the ligand fitted on the 001 surfaces of the crystal lattice. The binding on the 001 surfaces was also observed for other heme inhibitors (Buller et al. 2002; Ishmail et al. 2021; L'abbate et al. 2018; Veale et al. 2020). The interaction on this surface is possible mainly due to the planar nature of the inhibitors, which have conjugated aromatic moieties. Based on Biovia Discovery Studio's visualisation, non-covalent binding is the stabilization force for this ligand-heme adduct. The forces involved were π-π stacking and π-alkyl interactions between the indolyl moiety of the ligand and pyrrole rings or the alkyl group of the crystal hemozoin. Similarly, known

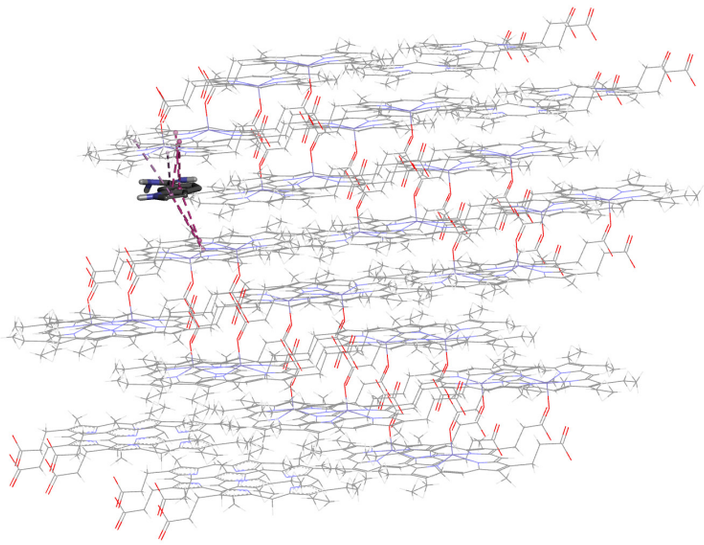

FIGURE 6. Docked conformation of hemozoin crystal with 6-amidinoindole at the {001} face of the hemozoin crystal

β-hematin or hemozoin inhibitor chloroquine also possesses π-π stacking interactions with the hemozoin (Bailly 2021). The interactions blocked the hemozoin polymerization and eventually prevented the heme's detoxification. The docking analysis supported that hemozoin inhibition could be the possible mechanism of action of this new heme binder. The study also supported the above heme binding experiments, demonstrating interactions between heme and ligand. However, *in vitro* and *in vivo* analyses are required to establish the mode of action between ligand and heme.

Conclusions

In summary, new compound, 6-amidinoindole has been successfully synthesized and characterized. The interaction of heme and ligand 6-amidinoindole was studied using absorption spectroscopy and molecular docking analysis. The heme-ligand association constant (log K) was 3.90 and the docking score was -8.3 kcal/mol. The results indicated that new 6-amidinoindole able to target and interact with malaria parasite through π-π stacking and π-alkyl interactions. In addition, with regards to the good affinities toward the hemozoin, it confirmed the potential of the ligand as the new heme binder. The findings also provide a basis for the mode of action between heme and ligand. Therefore, it was suggested to performed *in vitro* and *in vivo* analyses in the future in order to understand the compound's biological activity in depth.

Acknowledgements

The authors thank the Ministry of Higher Education (MOHE), Malaysia for funding under the Fundamental Research Grant Scheme (FRGS/1/2022/STG04/UKM/02/4) and University Kebangsaan Malaysia for providing facilities..

References

Alagona, G., Ghio, C. & Monti, S. 1998. The effect of small substituents on the properties of indole. An *ab initio* 6-31g* study. *Journal of Molecular Structure: THEOCHEM* 433(1-3): 203-216.

Ashley, E.A., Dhorda, M., Fairhurst, R.M., Amaratunga, C., Lim, P., Suon, S., Sreng, S., Anderson, J.M., Mao, S., Sam, B., Sopha, C., Chuor, C.M., Nguon, C., Sovannaroth, S., Pukrittayakamee, S., Jittamala, P., Chotivanich, K., Chutasmit, K., Suchatsoonthorn, C., Runcharoen, R., Hien, T.T., Thuy-Nhien, N.T., Thanh, N.V., Phu, N.H., Htut, Y., Han, K.T., Aye, K.H., Mokuolu, O.A., Olaosebikan, R.R., Folaranmi, O.O., Mayxay, M., Khanthavong, M., Hongvanthong, B., Newton, P.N., Onyamboko, M.A., Fanello, C.I., Tshefu, A.K., Mishra, N., Valecha, N., Phyo, A.P., Nosten, F., Yi, P., Tripura, R., Borrmann, S., Bashraheil, M., Peshu, J., Faiz, M.A., Ghose, A., Hossain, M.A., Samad, R., Rahman, M.R., Hasan, M.M., Islam, A., Miotto, O., Amato, R., MacInnis, B., Stalker, J., Kwiatkowski, D.P., Bozdech, Z., Jeeyapant, A., Cheah, P.Y., Sakulthaew, T., Chalk, J., Intharabut, B., Silamut, K., Lee, S.J., Vihokhern, B., Kunasol, C., Imwong, M., Tarning, J., Taylor, W.J., Yeung, S., Woodrow, C.J., Flegg, J.A., Das, D., Smith, J., Venkatesan, M., Plowe, C.V., Stepniewska, K., Guerin, P.J., Dondorp, A.M., Day, N.P., White, N.J. & Tracking Resistance to Artemisinin Collaboration (TRAC). 2014. Spread of artemisinin resistance in *Plasmodium falciparum* malaria. *New England Journal of Medicine* 371(5): 411-423.

Bailly, C. 2021. Pyronaridine: An update of its pharmacological activities and mechanisms of action. *Biopolymers* 112(4): e23398.

Brunet, C., Antoine, R., Lemoine, J.R.M. & Dugourd, P. 2012. Soret band of the gas-phase ferri-cytochrome C. *The Journal of Physical Chemistry Letters* 3(6): 698-702.

Buller, R., Peterson, M.L., Almarsson, O. & Leiserowitz, L. 2002. Quinoline binding site on malaria pigment crystal: A rational pathway for antimalaria drug design. *Crystal Growth & Design* 2(6): 553-562.

Congdon, M., Fritzemeier, R.G., Kharel, Y., Brown, A.M., Serbulea, V., Bevan, D.R., Lynch, K.R. & Santos, W.L. 2021. Probing the substitution pattern of indole-based scaffold reveals potent and selective sphingosine kinase 2 inhibitors. *European Journal of Medicinal Chemistry* 212: 113121.

Coronado, L.M., Nadovich, C.T. & Spadafora, C. 2014. Malarial hemozoin: From target to tool. *Biochimica et Biophysica Acta (BBA)-General Subjects* 1840(6): 2032-2041.

De Villiers, K.A. & Egan, T.J. 2021. Heme detoxification in the malaria parasite: A target for antimalarial drug development. *Accounts of Chemical Research* 54(11): 2649-2659.

Egan, T.J., Mavuso, W.W., Ross, D.C. & Marques, H.M. 1997. Thermodynamic factors controlling the interaction of quinoline antimalarial drugs with ferriprotoporphyrin Ix. *Journal of Inorganic Biochemistry* 68(2): 137-145.

Fong, K.Y. & Wright, D.W. 2013. Hemozoin and antimalarial drug discovery. *Future Medicinal Chemistry* 5(12): 1437-1450.

Furrer, J. 2021. Old and new experiments for obtaining quaternary-carbon-only NMR spectra. *Applied Spectroscopy Reviews* 56(2): 128-142.

Gil, S., Hošek, T., Solyom, Z., Kümmerle, R., Brutscher, B., Pierattelli, R. & Felli, I.C. 2013. NMR spectroscopic studies of intrinsically disordered proteins at near-physiological conditions. *Angewandte Chemie* 125(45): 12024-12028.

Ishmail, F.Z., Melis, D.R., Mbaba, M. & Smith, G.S. 2021. Diversification of quinoline-triazole scaffolds with corms: Synthesis, *in vitro* and *in silico* biological evaluation against *Plasmodium falciparum*. *Journal of Inorganic Biochemistry* 215: 111328.

Kapishnikov, S., Hempelmann, E., Elbaum, M., Als-Nielsen, J. & Leiserowitz, L. 2021. Malaria pigment crystals: The achilles′ heel of the malaria parasite. *ChemMedChem* 16(10): 1515-1532.

Kaushik, N.K., Kaushik, N., Attri, P., Kumar, N., Kim, C.H., Verma, A.K. & Choi, E.H. 2013. Biomedical importance of indoles. *Molecules* 18(6): 6620-6662.

Kollipara, M.R., Sarkhel, P., Chakraborty, S. & Lalrempuia, R. 2003. Synthesis, characterization and molecular structure of a new (?^{6}-P-Cymene) Ruthenium (II) amidine complex, [(?^{6}-P-Cymene)Ru{NH=C(Me)3,5-Dmpz}(3,5-Hdmpz)] $(BF_4)_2 \cdot H_2O$. *Journal of Coordination Chemistry* 56(12): 1085-1091.

Kumar, N., Singh, R. & Rawat, D.S. 2012. Tetraoxanes: Synthetic and medicinal chemistry perspective. *Medicinal Research Reviews* 32(3): 581-610.

L'abbate, F.P., Müller, R., Openshaw, R., Combrinck, J.M., De Villiers, K.A., Hunter, R. & Egan, T.J. 2018. Hemozoin inhibiting 2-phenylbenzimidazoles active against malaria parasites. *European Journal of Medicinal Chemistry* 159: 243-254.

Melo, M.N., Pereira, F.M., Rocha, M.A., Ribeiro, J.G., Junges, A., Monteiro, W.F., Diz, F.M., Ligabue, R.A., Morrone, F.B. & Severino, P. 2021. Chitosan and chitosan/peg nanoparticles loaded with indole-3-carbinol: Characterization, computational study and potential effect on human bladder cancer cells. *Materials Science and Engineering: C* 124: 112089.

Momma, K. & Izumi, F. 2008. Vesta: A three-dimensional visualization system for electronic and structural analysis. *Journal of Applied Crystallography* 41(3): 653-658.

Newman, D.J. & Cragg, G.M. 2007. Natural products as sources of new drugs over the last 25 years. *Journal of Natural Products* 70(3): 461-477.

Olafson, K.N., Nguyen, T.Q., Rimer, J.D. & Vekilov, P.G. 2017. Antimalarials inhibit hematin crystallization by unique drug-surface site interactions. *Proceedings of the National Academy of Sciences* 114(29): 7531-7536.

Omar, F., Tareq, A.M., Alqahtani, A.M., Dhama, K., Sayeed, M.A., Emran, T.B. & Simal-Gandara, J. 2021. Plant-Based indole alkaloids: A comprehensive overview from a pharmacological perspective. *Molecules* 26(8): 2297.

Openshaw, R., Maepa, K., Benjamin, S.J., Wainwright, L., Combrinck, J.M., Hunter, R. & Egan, T.J. 2021. A diverse range of hemozoin inhibiting scaffolds act on *Plasmodium falciparum* as heme complexes. *ACS Infectious Diseases* 7(2): 362-376.

Paloque, L., Ramadani, A.P., Mercereau-Puijalon, O., Augereau, J.M. & Benoit-Vical, F. 2016. *Plasmodium falciparum*: Multifaceted resistance to artemisinins. *Malaria Journal* 15(1): 1-12.

Pindur, U. & Lemster, T. 2001. Advances in marine natural products of the indole and annelated indole series: Chemical and biological aspects. *Current Medicinal Chemistry* 8(13): 1681-1698.

Radzuan, N.H.M., Norazmi, N.A.Z., Ali, A.H., Abu Bakar, M., Agustar, H.K., Abd Razak, M.R.M. & Hassan, N.I. 2021. Synthesis, *in vitro* antiplasmodial activity and cytotoxicity of metalloporphyrins against *Plasmodium falciparum* K1 strain. *Sains Malaysiana* 50(10): 2945-2956.

Roman, G., Rahman, M.N., Vukomanovic, D., Jia, Z., Nakatsu, K. & Szarek, W.A. 2010. Heme oxygenase inhibition by 2-Oxy-substituted 1-azolyl-4-phenylbutanes: Effect of variation of the azole moiety. x-ray crystal structure of human heme oxygenase-1 in complex with 4-phenyl-1-(1h-1, 2, 4-triazol-1-yl)-2-butanone. *Chemical Biology & Drug Design* 75(1): 68-90.

Sahyoun, T., Arrault, A. & Schneider, R. 2019. Amidoximes and oximes: Synthesis, structure, and their key role as no donors. *Molecules* 24(13): 2470.

Sam, J., Shamsusah, N.A., Ali, A.H., Hod, R., Hassan, M.R. & Agustar, H.K. 2022. Prevalence of simian malaria among macaques in Malaysia (2000-2021): A systematic review. *PLOS Neglected Tropical Diseases* 16(7): e0010527.

Srivastava, R.M., Pereira, M.C., Faustino, W.W., Coutinho, K., Dos Anjos, J.V. & De Melo, S.J. 2009. Synthesis, mechanism of formation, and molecular orbital calculations of arylamidoximes. *Monatshefte für Chemie-Chemical Monthly* 140(11): 1319-1324.

Stephenson, L., Warburton, W. & Wilson, M. 1969. Reaction of some aromatic nitriles with hydroxylamine to give amides, and an alternative preparation of amidoximes. *Journal of the Chemical Society C: Organic* 6: 861-864.

Taher, M., Razali, N.F.M., Susanti, D., Rahman, M.A. & Ade, M. 2022. Phytochemical constituents and pharmacological activities of *Picrasma javanica*: Quassinoids interest. *Sains Malaysiana* 51(3): 757-774.

Takahashi, O., Masuda, Y., Muroya, A. & Furuya, T. 2010. Theory of docking scores and its application to a customizable scoring function. *SAR and QSAR in Environmental Research* 21(5-6): 547-558.

Turner, H. 2016. Spiroindolone NITD609 is a novel antimalarial drug that targets the P-type ATPase PfATP4. *Future Medicinal Chemistry* 8(2): 227-238.

Veale, C.G., Jayram, J., Naidoo, S., Laming, D., Swart, T., Olivier, T., Akerman, M.P., De Villiers, K.A., Hoppe, H.C. & Jeena, V. 2020. Insights into structural and physicochemical properties required for β-hematin inhibition of privileged triarylimidazoles. *RSC Medicinal Chemistry* 11(1): 85-91.

Villarreal, W., Castro, W., González, S., Madamet, M., Amalvict, R., Pradines, B. & Navarro, M. 2022. Copper (I)-Chloroquine complexes: Interactions with DNA and ferriprotoporphyrin, inhibition of β-hematin formation and relation to antimalarial activity. *Pharmaceuticals* 15(8): 921.

Vörös, A., Mucsi, Z., Baán, Z., Timári, G., Hermecz, I., Mizsey, P. & Finta, Z. 2014. An experimental and theoretical study of reaction mechanisms between nitriles and hydroxylamine. *Organic & Biomolecular Chemistry* 12(40): 8036-8047.

*Corresponding author; email: aishah80@ukm.edu.my